to the ideal behavior. The termination of the antenna will result in ringing behavior that should be smoothed by an appropriate loading scheme. A partially focused monocone antenna would provide an omnidirectional radiator with the properties of (6), while a partially focused TEM horn would provide one with more gain. The antenna designed by Ameya, *et al.*, seems to accomplish this task by tapering the impedance of the printed monocone.

VI. Conclusion

In this paper we have presented requirements for an UWB antenna that can provide a dispersionless channel when used as both the transmit and receive antenna. The desired antenna would need to closely approximate an ideal, pulsed line source and would radiate a waveform that approximates a half derivative of the applied voltage. We demonstrated that such a waveform could be generated by a current source that is spatially limited by a Gaussian waveform.

Creating an antenna that produces such a pulse is a challenge. We provided a concept that might lead to such an antenna. By noting that a focused aperture antenna radiates a derivative of the applied voltage and a completely unfocused aperture radiates a replica of the applied voltage [4], it was hypothesized that an antenna that is focused in elevation but unfocused in azimuth would create the desired waveform, at least in the vicinity of the antenna. Further analysis of the proposed strategy is warranted. However, recent experimental results using printed monopole antennas seem to indicate that the desired goal can be achieved, at least over a limited range of frequencies [9].

Acknowledgment

The author is grateful to C. J. Buchenauer for numerous fruitful discussions about the concepts presented in this paper, and would like to thank R. Ziolkowski for his comments on the early versions of this manuscript.

References

[1] Z. N. Chen, X. H. Wu, H. F. Li, N. Yang, and M. Y. W. Chia, "Considertations for source pulses and antennas in UWB radio systems," *IEEE Trans. Antennas Propag.*, vol. 52, pp. 1739–1748, Jul. 2004.

[2] T. K. Sarkar, S. Burintramara, N. Yilmazer, S. Hwang, Y. Zhang, A. De, and M. Salazar-Palma, "A discussion about some of the principles/practices of wireless communication under a Maxwellian framework," *IEEE Trans. Antennas Propag.*, vol. 54, pp. 3727–3745, Dec. 2006.

[3] J. R. Andrews, "UWB signal sources, antennas and propagation," Application Note AN-14a, Picosecond Pulse Lab,. Boulder, CO, Aug. 2003 [Online]. Available: http://www.picosecond.com/objects/AN-14a.pdf/

[4] C. J. Buchenauer, J. S. Tyo, and J. S. H. Schoenberg, "Antennas and electric field sensors for ultra-wideband transient measurements: Applications and methods," in *Ultra-Wideband, Short-Pulse Electromagnetics 3*, C. E. Baum, L. Carin, and A. P. Stone, Eds. New York: Plenum, 1997, pp. 405–421.

[5] C. E. Baum, "General properties of antennas," in *Sensor and Simulation Notes #330*. Albuquerque, NM: Phillips Laboratory, 1991.

[6] M. Kanda, "The effects of resitive loading of TEM horns," *IEEE Trans. Electromagn. Compat.*, vol. 24, pp. 245–255, May 1982.

[7] C. E. Baum, E. G. Farr, and D. V. Giri, "Review of impulse-radiating antennas," in *Review of Radio Science*, W. R. Stone, Ed. New York: Oxford Univ. Press, 1999, pp. 403–439.

[8] N. Engheta, "On fractional calculus and fractional multipoles in electromagnetism," *IEEE Trans. Antennas Propag.*, vol. 44, pp. 554–566, Apr. 1996.

[9] M. Ameya, M. Yamamoto, and T. Nojima, "An omnidirectional UWB printed dipole antenna with small waveform distortion," in *Proc. Progress In Electromagnetics Research Symp PIERS 2006*, Tokyo, Japan, Aug. 2006, p. 515.

A MIMO Channel Model Based on the Nakagami-Faded Spatial Eigenmodes

Michail Matthaiou, David I. Laurenson, and John S. Thompson

***Abstract*—We propose a stochastic model for multiple-input multiple-output (MIMO) communication systems based on the eigendecomposition of the spatial correlation matrix. It is shown that the channel matrix can be well modeled by the superposition of the spatial eigenmodes experiencing independent Nakagami-m fading. The proposed scheme is also compared with the existing correlation-based models using the data obtained from an indoor measurement campaign so that its performance is assessed in depth.**

***Index Terms*—Fading channels, multiple-input multiple-output (MIMO) systems, spatial correlation.**

I. Introduction

In recent years, the area of multiple-input multiple-output (MIMO) channel modeling has attracted considerable research interest since a reliable model can in principle predict the propagation mechanisms and ultimately make possible the integration of MIMO technology into real-time applications. On this basis, various stochastic modeling approaches have been proposed in the literature with a view to capturing the spatial behavior at both the transmitter (Tx) and the receiver (Rx).

More specifically, the so called "Kronecker model" [1] assumes that the spatial correlation properties at both ends of the link are separable which can result though in the multipath structure being rendered incorrectly. In other words, it enforces the joint angular power spectrum (APS) to be the product of the direction of arrival (DoA) and direction of departure (DoD) power spectra. The model may give accurate estimates when three or less antenna elements are employed but for larger arrays (and hence an improved angular resolution) its performance deteriorates significantly [2]. However, it has been extensively used for the theoretical analysis and simulations of MIMO systems thanks to its simplicity.

On the other hand, the so called "Weichselberger model" [3] alleviates the deficiencies of the Kronecker model by considering the joint correlation structure of both ends and consequently the average coupling between the spatial subchannels is effectively modeled. Although more robust than the Kronecker model with systems employing more than four antennas, it still falls short of precisely capturing all spatial activity [4], [5]. Yet, the multipath environment is occasionally not reproduced properly resulting in an inaccurate estimate of the joint APS.

In this letter, we present a full spatial correlation model which encompasses a generalized version of the aforementioned approaches and yields a better fit, in terms of statistical metrics, with the measured data. The common assumption of Rayleigh fading, which is often violated in measured channels, is relaxed by considering the more flexible Nakagami-m distribution in order to account for the presence of strong obstructed line-of-sight (LoS) components.

The letter is organized as follows: In Section II, we derive the proposed MIMO channel model in a straightforward manner. In Section III, an indoor MIMO measurement campaign is described. The statistical characteristics as well as the accuracy of the Nakagami-m

Manuscript received May 8, 2007; revised December 17, 2007.

The authors are with the Institute for Digital Communications, Joint Research Institute for Signal and Image Processing, School of Engineering and Electronics, The University of Edinburgh, EH9 3JL, Edinburgh, U.K. (e-mail: M.Matthaiou@ed.ac.uk).

Digital Object Identifier 10.1109/TAP.2008.922708

fading assigned to each eigenmode are addressed in Section IV. The performance of the stochastic model is evaluated in Section V using the measured data. Finally, Section VI summarizes the key findings.

II. MIMO Channel Model

For a flat-fading MIMO system equipped with N transmit and M receive antenna elements, the complex input-output relationship can be written for the discrete case as

$$\mathbf{y} = \mathbf{H}\mathbf{x} + \mathbf{n} \tag{1}$$

where $\mathbf{x} \in \mathbb{C}^{N\times 1}$ is the transmitted signal vector, $\mathbf{y} \in \mathbb{C}^{M\times 1}$ is the noise-corrupted received signal and $\mathbf{n} \in \mathbb{C}^{M\times 1}$ corresponds to the additive noise plus interference. The term $\mathbf{H} \in \mathbb{C}^{M\times N}$ is usually referred to as the channel transfer function matrix and contains the complex responses between all antenna pairs. The full spatial correlation matrix, describing the joint correlation properties of both link ends, is defined as [1]

$$\mathbf{R}_{\mathbf{H}} \triangleq E_{\mathbf{H}}\{\mathrm{vec}(\mathbf{H})\mathrm{vec}(\mathbf{H})^H\} \in \mathbb{C}^{MN\times MN} \tag{2}$$

where the vec$(\cdot)$ operator stacks the columns of a matrix into a vector and $(\cdot)^H$ is the Hermitian transposition. The eigendecomposition of $\mathbf{R}_{\mathbf{H}}$ into a sum of rank-one matrices yields

$$\mathbf{R}_{\mathbf{H}} = \sum_{k=1}^{MN} \lambda_k \mathbf{u}_k \mathbf{u}_k^H \tag{3}$$

where λ_k are the real non zero ordered eigenvalues ($\lambda_1 \geq \lambda_2 \geq \cdots \geq \lambda_{MN} \geq 0$) and $\mathbf{u}_k$ contain the corresponding eigenvectors which are by definition mutually orthogonal and have unit norm. We note that the number of non-zero eigenvalues determines the rank of $\mathbf{R}_{\mathbf{H}}$ which is upper bounded by MN. The eigenvector $\mathbf{u}_k$ can be reshaped column-wise into the matrix $\mathbf{U}_k = \mathrm{unvec}(\mathbf{u}_k) \in \mathbb{C}^{M\times N}$ which we will refer to hereafter as the k-th *eigenmode*. From a physical viewpoint, eigenvalues specify the degree of diversity offered by the channel while eigenmodes, commonly representing a linear combination of propagation paths, are indicative of the spatial multiplexing (SM) ability [3]. Likewise, the channel matrix can be modeled as

$$\mathbf{H}_{\mathrm{mod}} = \sum_{k=1}^{MN} g[k]\sqrt{\lambda_k}\mathbf{U}_k. \tag{4}$$

From (4), we readily infer that the probability density function (pdf) of $g[k]$ expresses the fading variations of the channel. In fact, the fading coefficients $g[k]$ are independent and identically distributed (i.i.d.) random variables satisfying the relationship $E_g\{g[m]g^*[n]\} = \delta_{mn}$, where δ_{mn} is the Kronecker delta function.[1] We underline the fact that the second-order moment of $g[k]$ is assumed to be the same for all k so that the eigenvalues λ_k reflect the power of each eigenmode.

III. Indoor Measurement Campaign

An indoor measurement campaign was carried out in the Electrical Engineering Building in Vienna University of Technology [6]. The measurements were conducted using the MEDAV RUSK ATM channel sounder which was probed at 193 equispaced frequency bins, covering 120 MHz of bandwidth, at a carrier frequency of 5.2 GHz. The Rx employed a uniform linear array (ULA) of eight vertically-polarized elements with an inter-element distance of 0.4λ which was fully calibrated in order to remove the undesired effects of mutual coupling and other array imperfections. At the Tx, an omnidirectional sleeve antenna was moved on a 10×20 rectangular grid with element spacings of 0.5λ. By considering a virtual eight-element ULA on each row, we end up with $13 \times 10 = 130$ spatial realizations of the 8×8 MIMO transfer matrix. Thus, a total set of $130 \times 193 = 25,090$ space and frequency realizations per measurement scenario was obtained.

The Rx was placed at 24 locations in several offices while the Tx was fixed in a hallway. In order to capture the whole azimuth domain activity, the Rx was steered to three different directions (spaced by 120°), leading to the generation of 72 data sets, i.e., combinations of Rx positions and directions.

IV. Nakagami-M Fading Characteristics

Intuitively, the main concept behind the proposed model (4) originates from the well-known *Karhunen-Loeve transform* (KLT) which has been extensively used in numerous applications that range from image compression to seismology and computer graphics in order to decorrelate multi-element data based on the eigendecomposition of the correlation matrix [7]. The resulting uncorrelated eigenmodes are assigned a Nakagami-m fading process [8] which yields a satisfactory fit with real-time data for various measured channels (see [9] and references therein). The normalized Nakagami-m pdf of the fading envelope R is given by

$$f_R(r) = \frac{2}{\Gamma(m)} m^m r^{2m-1} e^{-mr^2}, \quad r \geq 0 \tag{5}$$

with $\Gamma(\cdot)$ expressing the gamma function. The Nakagami fading figure $m[k] (1 \leq k \leq MN)$, which determines the severity of fading, is estimated directly from the measured data according to

$$\begin{aligned} m[k] &= \frac{E\left\{\left|\mathbf{u}_k^H \mathrm{vec}(\mathbf{H})\right|^2\right\}^2}{E\left\{\left\{\left|\mathbf{u}_k^H \mathrm{vec}(\mathbf{H})\right|^2 - E\left\{\left|\mathbf{u}_k^H \mathrm{vec}(\mathbf{H})\right|^2\right\}\right\}^2\right\}} \\ &= \frac{\lambda_k^2}{E\left\{\left\{\left|\mathbf{u}_k^H \mathrm{vec}(\mathbf{H})\right|^2 - \lambda_k\right\}^2\right\}} \geq \frac{1}{2}. \end{aligned} \tag{6}$$

In Fig. 1, we illustrate the cumulative distribution function (cdf) of a normalized measured fading envelope which indicates the excellent fit of the Nakagami-m distribution.

This aggregate statistical metric shows the poor match of the commonly used Rayleigh distribution while the Ricean distribution fits reasonably well, except in the tails of the measured data. Similar trends were observed at most of the considered cases. To further justify our choice, we have computed the mean squared error (MSE) of these three candidate cdf fits across the whole data set with the key characteristics being tabulated in Table I. The average and standard deviation measures indicate that the Nakagami-m fit yields a rather good accuracy and substantially outperforms the Rayleigh fit by an order of one magnitude while it remains robust and experiences the lowest maximum MSE. On the basis of which model best fits the measured data set, we notice the smallest MSE to occur at 72.40% of the cases when a Nakagami-m fit is employed thereby confirming its improved performance compared to the other two reference distributions (right-hand column of Table I). For the generation of the uncorrelated Nakagami-m

[1]It is trivial to check the validity of (4) by calculating the spatial correlation matrix according to (2).

TABLE I
MSE CHARACTERISTICS OF THREE CDF FITTING DISTRIBUTIONS

	average MSE	std. deviation MSE	minimum MSE	maximum MSE	smallest MSE
Rayleigh	2.38×10^{-4}	1.72×10^{-3}	5.59×10^{-7}	5.32×10^{-2}	5.79 (%)
Ricean	4.95×10^{-5}	1.28×10^{-4}	5.53×10^{-7}	4.72×10^{-3}	21.81 (%)
Nakagami-m	3.81×10^{-5}	1.23×10^{-4}	4.65×10^{-7}	4.18×10^{-3}	72.40 (%)

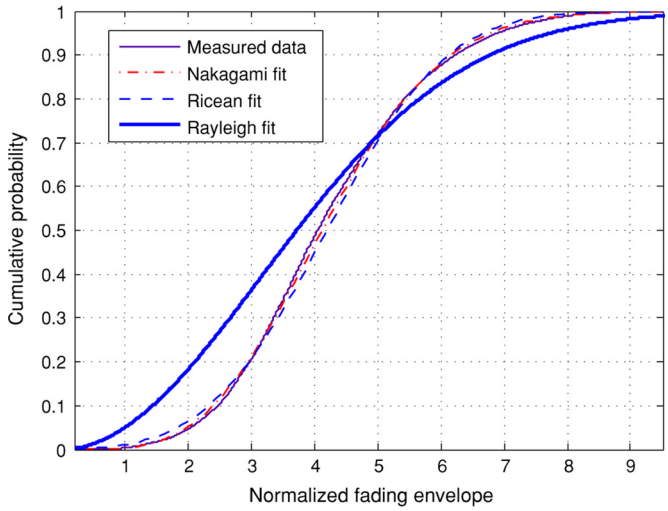

Fig. 1. Cdf of a normalized measured envelope in comparison with Nakagami-m, Ricean and Rayleigh distributions.

envelope variates we adopt the *rejection/acceptance method* proposed in [10] which is accurate and computationally efficient for arbitrary values of m. Then, the spatial fading coefficients may be expressed as $g[k] = R[k]\exp(j\,\phi[k])$, where $\phi[k]$ is a random phase distributed uniformly in $[0, 2\pi)$. The uniform phase assumption was found to be valid even for large values of the m-factor (i.e., non-Rayleigh conditions) and thanks to its intrinsic simplicity was incorporated throughout our analysis.

V. MIMO CHANNEL MODEL VALIDATION

The proposed model is assessed by means of the mutual information and the link-level performance using a minimum mean squared error (MMSE) detector which can minimize the overall error caused by noise and mutual interference. Firstly, we compute the measured correlation matrix, using all space and frequency realizations, and thereafter the matrix is decomposed in order to obtain the spatial eigenmodes; as a next step 25,090 synthetic channel realizations are generated according to (4) and hence the measured and simulated ensembles are the same. In order to remove the path-loss effects, both ensembles are normalized so that the constraint $E\{\|\mathbf{H}\|_F^2\} = MN$ is fulfilled, where $\|\cdot\|_F$ corresponds to the Frobenius norm.

Assuming perfect channel state information (CSI) at the Rx but no knowledge at the Tx, the average mutual information (ergodic channel capacity) is given by

$$I = E\left\{\log_2\left(\det\left(\mathbf{I}_M + \frac{\rho}{N}\mathbf{H}\mathbf{H}^H\right)\right)\right\}, \qquad (\text{bits/s/Hz}) \quad (7)$$

where $\mathbf{I}_M$ is the $M \times M$ identity matrix and ρ denotes the system signal-to-noise ratio (SNR) per receiver branch [11]. The latter was set equal to 20 dB[2] while the expectation operation was performed on either the measured data or the fading realizations of $g[k]$. In Fig. 2, two different models are compared, namely the Nakagami and the Weichselberger models; the modeled capacity is plotted against the measured capacity for each of the 72 scenarios under investigation. The Kronecker model is not included in our comparison since it is a special case of the Weichselberger model and yields an inferior performance for the great majority of cases [3]–[5].

From this figure, we observe that the proposed model holds a smaller modeling error than the Weichselberger model, whose mismatch increases with decreasing mutual information, for all the scenarios under investigation; in particular, a 2.2 dB improvement was achieved in the MSE from -9.72 to -11.93 dB. Additional study revealed that the Weichselberger's accuracy diminishes when the outage mutual information is considered, resulting in an overestimation of the diversity level; this is consistent with the results presented in [4], [5]. The good fit of the Nakagami model can be partially attributed to the presence of strong obstructed LoS components at the majority of Rx locations due to its inherent higher flexibility compared to the more restricted Rayleigh and Ricean distributions. In other words, for the corresponding eigenmodes $m > 1$ and therefore the fluctuations of the signal strength reduce compared to Rayleigh fading.

The link-level performance is evaluated by considering a SM scheme, namely linear MMSE detection. The uncoded transmitted signal is modulated using BPSK modulation. For these specifications, the estimated transmit signal vector $\hat{\mathbf{x}}$ is [12]

$$\hat{\mathbf{x}} = \widetilde{\mathbf{W}} \cdot \mathbf{y}, \text{ where } \widetilde{\mathbf{W}} = \arg\min_{\mathbf{W}} E\{\|\mathbf{W}\mathbf{y} - \mathbf{x}\|^2\} \qquad (8)$$

and thus the following closed-form expression is finally obtained

$$\hat{\mathbf{x}} = \mathbf{H}^H(\mathbf{H}\mathbf{H}^H + N_0\mathbf{I}_M)^{-1} \cdot \mathbf{y} \qquad (9)$$

with N_0 expressing the noise power. Due to space constraints, we directly focus on the *BER mismatch* at a target SNR of 20 dB against the Nakagami m-factor of the dominant eigenmode (cf. Fig. 3). In general, the BER mismatch is defined as the difference between the measured and the modeled BER at a target SNR. The distribution of the m values validates clearly the assumption of Nakagami fading while we notice a significant portion of them well beyond the typical unity value. The proposed model holds again a superior performance for the vast majority of measured scenarios (68 out of 72 scenarios); in fact, its BER estimators deviate by up to 11% while the Weichselberger's by up to 20% and the MSEs (for the same target SNR) are 2.24×10^{-5} and 4.47×10^{-5} respectively, expressing a 3 dB improvement. It is noteworthy that the relative difference of estimators is higher when more than one eigenmodes experience purely Nakagami fading ($m > 2$).

The only disadvantage of the proposed scheme lies in its increased complexity burden which is generally a crucial issue that affects the choice of the most appropriate channel model. While the Kronecker

[2]This value is chosen so that the system SNR is well below the measured SNR which lies in the region 55-60 dB after averaging the channel response across 128 temporal snapshots.

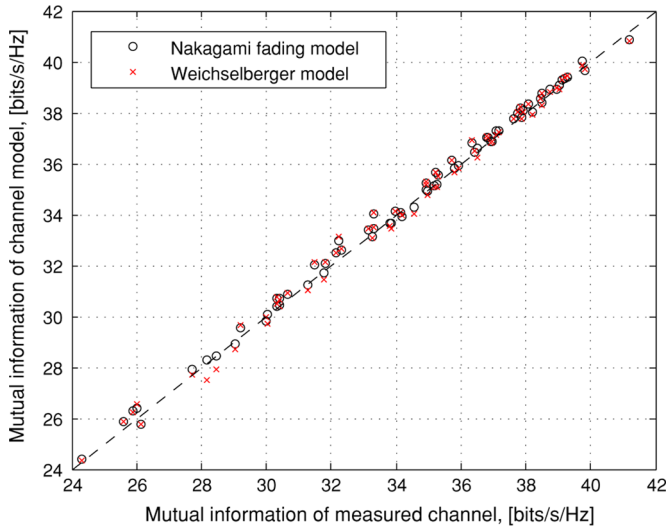

Fig. 2. Mutual information for two different channel models versus measured mutual information. The dashed line corresponds to the points of no modeling error.

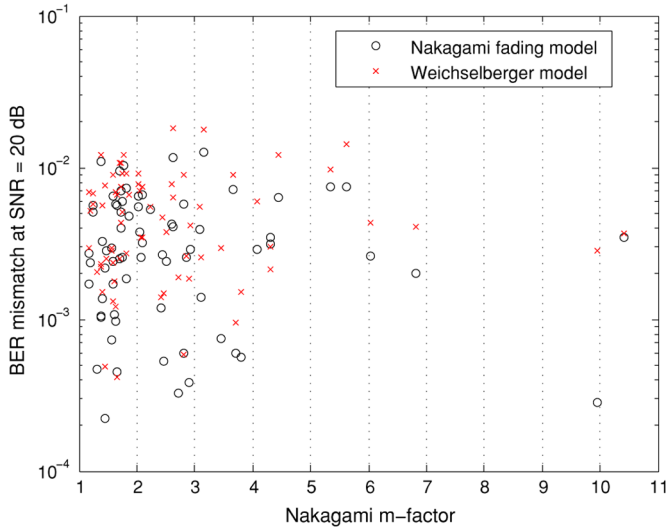

Fig. 3. BER mismatch at a target SNR of 20 dB against the Nakagami $\boldsymbol{m}$-factor of the dominant eigenmode.

and the Weichselberger models require respectively $M^2 + N^2 = 128$ and $MN + M(M-1) + N(N-1) = 176$ real parameters to be specified, the complexity order of our scheme is equal to that of the full correlation model, i.e., $(MN)^2 = 4096$. This implies that for practical systems of interest the complexity increase is modest; further, in terms of processing time an increase of 45% was observed on a 3.2 GHz Pentium, making the model rather appealing when an enhanced accuracy is desired.

VI. Conclusion

In this letter, a stochastic channel model has been presented with a view to the decomposition of the spatial correlation matrix. The Nakagami-m fading approach yields a satisfactory performance since in the majority of measured locations the presence of strong obstructed LoS components violates the common assumption of Rayleigh fading conditions. It is shown that the proposed model outperforms the sophisticated Weichselberger model in terms of both information theory (mutual information) and link-level performance (BER). The scheme can be regarded as a framework for describing different channels operating at the 5 GHz frequency band, e.g., Wireless Local Area Networks (WLANs), fixed wireless and peer-to-peer communications. It can also be used as a tractable tool for the simulation of MIMO systems, design of space-time codes and construction of spatial filtering at both ends.

Acknowledgment

The authors would like to thank Dr. M. Herdin, formerly of TU Vienna, for providing them with access to the results of propagation measurements carried out in Vienna. They would also like to acknowledge the support of the Scottish Funding Council for the Joint Research Institute with the Heriot-Watt University which is a part of the Edinburgh Research Partnership.

References

[1] J. P. Kermoal, L. Schumacher, K. I. Pedersen, P. E. Mogensen, and F. Frederiksen, "A stochastic MIMO radio channel model with experimental validation," *IEEE J. Sel. Areas Commun.*, vol. 20, pp. 1211–1226, Aug. 2002.

[2] H. Özcelik, M. Herdin, W. Weichselberger, J. Wallace, and E. Bonek, "Deficiencies of "Kronecker" MIMO radio channel model," *IEE Electron. Lett.*, vol. 39, no. 16, pp. 1209–1210, Aug. 2003.

[3] W. Weichselberger, "Spatial structure of multiple antenna radio channels: a signal processing viewpoint," Ph.D. dissertation, Technical Univ. Vienna, Austria, Dec. 2003.

[4] H. Özcelik, N. Czink, and E. Bonek, "What makes a good MIMO channel model?," in *Proc. VTC 2005*, May 2005, vol. 1, pp. 156–160.

[5] H. Özcelik, "Indoor MIMO channel models," Ph.D. dissertation , Technical Univ. Vienna, Austria, Dec. 2004.

[6] M. Herdin, H. Özcelik, H. Hofstetter, and E. Bonek, "Variation of measured indoor MIMO capacity with receive direction and position at 5.2 GHz," *IEE Electron. Lett.*, vol. 38, no. 21, pp. 1283–1285, Oct. 2002.

[7] S. Theodoridis and K. Koutroumbas, *Pattern Recognition*, 2nd ed. New York: Academic Press, 2003.

[8] M. Nakagami, W. C. Hoffman, Ed., "The $\boldsymbol{m}$-distribution—A general formula of intensity distribution of rapid fading," in *Statistical Methods in Radio Wave Propagation*, Oxford, U.K., 1960, pp. 3–36.

[9] P. J. Crepeau, "Uncoded and coded performance of MFSK and DPSK in Nakagami fading channels," *IEEE Trans. Commun.*, vol. 40, pp. 487–493, Mar. 1992.

[10] L. Cao and N. C. Beaulieu, "A simple efficient method for generating independent Nakagami-$\boldsymbol{m}$ fading samples," *Proc. VTC 2005*, pp. 44–47, Jun. 2005.

[11] G. Foschini and M. Gans, "On limits of wireless communication in a fading environment when using multiple antennas," *Wireless Pers. Commun.*, vol. 6, no. 3, pp. 311–335, Feb. 1998.

[12] S. Haykin, *Adaptive Filter Theory*, 4th ed. Englewood Cliffs, NJ: Prentice Hall, 2001.